Chemistry & Biology, Vol. 12, 357–369, March, 2005, ©2005 Elsevier Ltd All rights reserved. DOI 10.1016/j.chembiol.2004.12.011

Delineation of the Chemical Pathways Underlying Nitric Oxide-Induced Homologous Recombination in Mammalian Cells

Tanyel Kiziltepe,[1,2] Amy Yan,[2] Min Dong,[2] Vidya S. Jonnalagadda,[2] Peter C. Dedon,[2] and Bevin P. Engelward[2,*]
[1]Department of Chemistry
Massachusetts Institute of Technology
Cambridge, Massachusetts 02139
[2]Biological Engineering Division
Massachusetts Institute of Technology
Cambridge, Massachusetts 02139

Summary

Inflammation is an important risk factor for cancer. During inflammation, macrophages secrete nitric oxide ($NO^{\bullet}$), which reacts with superoxide or oxygen to create $ONOO^-$ or N_2O_3, respectively. Although homologous recombination causes DNA sequence rearrangements that promote cancer, little was known about the ability of $ONOO^-$ and N_2O_3 to induce recombination in mammalian cells. Here, we show that $ONOO^-$ is a potent inducer of homologous recombination at an integrated direct repeat substrate, whereas N_2O_3 is relatively weakly recombinogenic. Furthermore, on a per lesion basis, $ONOO^-$-induced oxidative base lesions and single-strand breaks are significantly more recombinogenic than N_2O_3-induced base deamination products, which did not induce detectable recombination between plasmids. Similar results were observed in mammalian cells from two different species. These results suggest that $ONOO^-$-induced recombination may be an important mechanism underlying inflammation-induced cancer.

Introduction

Nitric oxide ($NO^{\bullet}$) is a key mediator of diverse biological processes, including vasodilation, neurotransmission, endotoxic shock, cerebral ischemia, and inflammation [1–3]. At low concentrations, $NO^{\bullet}$ is involved in intra- and intercellular signaling, while at high concentrations, $NO^{\bullet}$ is toxic [4–6]. As a cytotoxic agent, $NO^{\bullet}$ is secreted by activated macrophages, along with oxygen radicals and other cytotoxic chemicals during the inflammatory response. Importantly, tissue inflammation associated with gastritis, hepatitis, and colitis is an important risk factor for a variety of human cancers, such as gastric cancer, liver cancer, and cholangiocarcinoma [7]. Furthermore, it is estimated that ~15% of cancer cases worldwide are attributable to infectious diseases, many of which induce chronic inflammation [8]. Although the underlying mechanism of inflammation-induced cancer is not yet fully understood, exposure of tissues to reactive oxygen and nitrogen species is thought to cause mutations and genetic rearrangements that contribute to tumor initiation and progression. While $NO^{\bullet}$-induced point mutations have been studied extensively (e.g., see references [9–11]), very little is known about the ability of $NO^{\bullet}$ to induce other classes of mutations, such as sequence rearrangements that are mediated by homologous recombination.

Mitotic homologous recombination allows cells to repair DNA double-strand breaks by extracting missing sequence information from a sister chromatid (during S and G2 phases of cell cycle) or from a homologous chromosome. In addition, homologous recombination plays a critical role in restoring collapsed forks during DNA replication (for excellent reviews of homologous recombination, see references [12–14]). Although homologous recombination is generally highly accurate, transfer of genetic material carries with it a finite risk of a deliterious rearrangement, since recombination between misaligned sequences can lead to insertions, deletions, inversions, and translocations. In addition, exchanges between homologous chromosomes are responsible for causing most spontaneous loss of heterozygosity events in mammals [15, 16]. Nearly all tumors carry sequence rearrangements that are likely the result of mitotic homologous recombination. Consequently, whether by exposure to endogenous and environmental recombinogens, or by inherited predisposition, conditions that lead to increased levels of homologous recombination are associated with an increased risk of cancer [17–19].

Very little is known about the recombinogenicity of $NO^{\bullet}$ and its derivative reactive nitrogen species in mammals. However, there are a few studies suggesting that $NO^{\bullet}$ may induce recombination in mammalian cells. For example, patients who suffer from chronic inflammation associated with Crohn's disease have increased levels of sister chromatid exchange (SCE) in their lymphocytes [20], though it is not known to what extent $NO^{\bullet}$ is responsible for this effect. In addition, two studies have shown that mammalian cells exposed to chemicals that give rise to $NO^{\bullet}$ ("$NO^{\bullet}$ donors") suffer increased levels of SCEs [21, 22], though the $NO^{\bullet}$ donors used in these studies also give rise to additional potentially recombinogenic radical species. The observation that mammalian cells exposed to $NO^{\bullet}$ have an increased susceptibility to loss of heterozygosity provides additional support for the possibility that $NO^{\bullet}$ induces recombination [23]. Taken together, these observations suggest that $NO^{\bullet}$ may induce homologous recombination in mammalian cells. Here, we set out to define the potential of $NO^{\bullet}$ to induce homologous recombination in mammalian cells, and to explore the underlying chemistry that might be responsible for its effects.

It is well established that the recombinogenicity of a DNA damaging agent is dependent on the types of DNA lesions that it induces. $NO^{\bullet}$ reacts with oxygen and superoxide to form N_2O_3 and $ONOO^-$, respectively, which are the dominant reactive nitrogen species formed under physiological conditions (Figure 1A). Although $NO^{\bullet}$ does not directly damage DNA, N_2O_3 is a potent DNA deaminating agent, and $ONOO^-$ is a potent DNA oxidizing agent. Most of the lesions created by N_2O_3 are base

*Correspondence: bevin@mit.edu

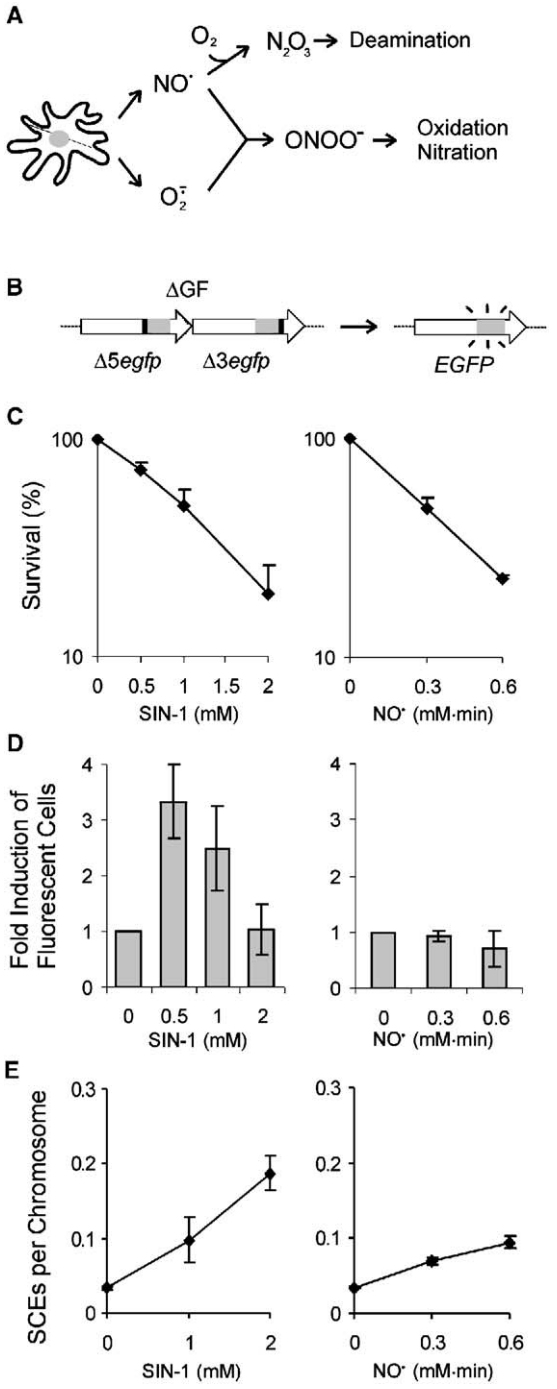

Figure 1. NO•/O_2- or SIN-1-Induced Toxicity and Homologous Recombination in Mouse Embryonic Stem Cells

(A) Schematic depicting the major reactions of NO• secreted by activated macrophages.

(B) The chromosomal direct repeat substrate. Expression cassettes are represented by large arrows with emphasis on the coding sequences (gray) and deleted regions (black). Δ5*egfp* and Δ3*egfp* expression are driven by the chicken β-actin promoter and cytomegalovirus enhancer. Homologous recombination can lead to the restoration of full-length *EGFP* coding sequence and fluorescence expression.

(C) Relative toxicity induced by exposure to the indicated doses of NO• delivered in the gas delivery chamber or SIN-1 as determined by colony forming assay. For NO• exposure, Ar gas was used as a negative control, and relative survival was normalized accordingly. Values are the mean of three samples ± SEM.

(D) Relative levels of damage-induced recombination at a chromosomally integrated direct repeat. Fold induction of fluorescent recombinant cells is shown. Following exposure to NO•/O_2 or SIN-1 (72 hr), cells were analyzed by flow cytometry. Values are the mean of three samples ± SEM.

(E) SCEs induced by SIN-1 and NO•/O_2. SCEs per chromosome were detected by analyzing 20 metaphase chromosomes at each dose. The results shown are mean ± SD for duplicate experiments.

damages, while $ONOO^-$ attacks both the base and sugar moieties of DNA [11]. For example, N_2O_3 deaminates DNA bases, creating lesions such as uracil, hypoxanthine, and xanthine [24–27], and $ONOO^-$ oxidation of guanine leads to 8-oxoguanine and its secondary oxidation products, 8-nitroguanine, as well as abasic sites formed by spontaneous depurination of 8-nitroguanine [27–31]. In addition to base lesions, $ONOO^-$ also directly induces direct single-strand breaks in DNA, by the oxidative breakdown of deoxyribose [29, 32, 33].

Although double-strand breaks are thought to be critical for inducing homologous recombination, in vitro studies using purified DNA have shown that neither N_2O_3, nor $ONOO^-$ efficiently creates double-strand breaks by direct reaction with DNA [32, 34, 35]. However, base lesions, abasic sites, and single-strand breaks can be converted into double-strand breaks by enzymatic processing (when in close proximity) or when they are encountered by the replication fork. For example, during base excision repair (BER), single-strand breaks are created as repair intermediates by DNA glycosylases that have an associated AP lyase activity and by AP endonucleases [36]. Consequently, if DNA glycosylases initiate BER of closely opposed lesions, double-strand breaks can be formed in vitro [37, 38]. Alternatively, DNA lesions that inhibit replication fork progression, such as BER intermediates, are highly recombinogenic in mammalian cells (e.g., see references [39, 40]). Indeed, previous work from this laboratory has demonstrated that DNA glycosylases promote NO•-induced recombination in *E. coli*, presumably by converting BER substrates into recombinogenic double-strand breaks [41]. Furthermore, studies in mammalian cells have recently shown that glycosylases promote radiation-induced strand breaks [42].

As a first step toward revealing the underlying mechanisms of NO•-induced sequence rearrangements in mammals, we set out to reveal the chemical basis for NO•-induced recombination in mammalian cells. Toward this end, we compared the recombinogenic effects of the two predominant reactive nitrogen species produced under physiological conditions: N_2O_3 and $ONOO^-$. For example, by exposing cells to NO• and O_2 gases simultaneously in a specially designed NO• gas delivery chamber [43], the major DNA damaging agent formed is N_2O_3. Alternatively, cells can be exposed to $ONOO^-$ using 3-morpholinosydnonimine (SIN-1), which produces equal amounts of superoxide and NO• that rapidly react to form $ONOO^-$. However, in the case of the NO• delivery chamber, due to the inevitable presence of intracellular superoxide, it is not possible to

completely eliminate formation of some $ONOO^-$. Similarly, due to the presence O_2 during SIN-1 exposure, it is not possible to eliminate the possibility that some N_2O_3 is formed. Thus the $NO^\bullet$ delivery chamber and SIN-1, which are amenable for studies of cultured cells, provide effective strategies for creating conditions that favor the formation of $ONOO^-$ or N_2O_3, although not with absolute purity. In contrast, in vitro conditions can be readily created in which plasmid DNA is virtually exclusively exposed to either N_2O_3 or $ONOO^-$. Therefore, the combined approaches of studying chromosomal recombination in cells exposed to conditions that favor formation of either N_2O_3 or $ONOO^-$, and studying plasmid recombination between DNA molecules exposed to conditions that give rise to exclusively N_2O_3 or $ONOO^-$, provide a powerful strategy for elucidating the chemical nature of $NO^\bullet$-induced recombination in mammalian cells.

Here, we show that exposure of mammalian cells to conditions that favor formation of N_2O_3 is relatively weakly recombinogenic, and that N_2O_3-induced DNA lesions fail to induce interplasmid recombination. In contrast, conditions that favored formation of $ONOO^-$ are highly recombinogenic, both when cells are exposed and when plasmid is exposed to $ONOO^-$ and subsequently transfected into cells. By quantifying strand breaks, abasic sites, and base lesions induced by N_2O_3 and $ONOO^-$ in plasmid DNA, we demonstrate that chemically induced strand breaks and oxidative base lesions are far more recombinogenic than deaminated base lesions, even under conditions where the quantity of N_2O_3-induced lesions exceeds that of $ONOO^-$-induced lesions. The results of these studies contribute to our understanding of the biological consequences of chronic inflammation and provide a framework for delineating conditions that are most likely to lead to tumorigenic sequence rearrangements in people.

Results

SIN-1, but Not $NO^\bullet/O_2$, Induces Homologous Recombination at a Chromosomally Integrated Direct Repeat

To study $NO^\bullet/O_2$-induced homologous recombination in mammalian cells, we used mouse embryonic stem cells that carry a direct repeat substrate that yields a fluorescent phenotype specifically as a result of mitotic homologous recombination events [44]. The ΔGF cells carry expression cassettes for two different truncated *egfp* cDNAs that are arranged in a direct repeat (Figure 1B; essential coding sequences were deleted from either the 5′ or the 3′ end to create Δ5*egfp* and Δ3*egfp*, respectively). In this system, recombination via several different mechanisms can reconstitute the full-length *EGFP* sequence (e.g., gene conversion, unequal sister chromatid exchanges, and replication fork repair [14]). Thus, recombination frequency can be readily estimated by quantifying green fluorescent recombinant cells by flow cytometry [44, 45].

To study the effects of $ONOO^-$ and N_2O_3, ΔGF cells were exposed to various concentrations of SIN-1 (to deliver $ONOO^-$) or to $NO^\bullet$ and O_2 gases delivered simultaneously via a Silastic tubing-based $NO^\bullet$ delivery chamber to deliver N_2O_3 (referred to as "$NO^\bullet/O_2$" exposure below) [43]. It is well established that for most DNA damaging agents, the frequency of recombination rises as the toxicity increases. Therefore, to compare the recombinogenic effects of $ONOO^-$ and N_2O_3, we established conditions that induce similar levels of cytotoxicity (Figure 1C). Cells were then exposed to equitoxic doses of SIN-1 or $NO^\bullet/O_2$ and were subsequently analyzed by flow cytometry to quantify fluorescent cells. As can be seen in Figure 1D, SIN-1 is clearly recombinogenic, inducing recombination up to ~3-fold. It is noteworthy that induction of recombination by SIN-1 initially increases and then decreases as a function of dose, an observation that has also been noted by others (e.g., reference [46]). In contrast to SIN-1, exposure to $NO^\bullet/O_2$ did not lead to any detectable increase in the frequency of recombinant cells (Figure 1D), even at doses that diminished survival to below 1% (data not shown). Thus, while SIN-1 induces recombination at a chromosomally integrated recombination substrate, $NO^\bullet/O_2$ does not.

SIN-1 Is a More Potent Inducer of SCEs than $NO^\bullet/O_2$

The chromosomal direct repeat assay offers a rapid and effective measure of recombination at a single locus. To assess recombination throughout the genome rather than at a single locus, we measured SCEs, which are known to result from homologous recombination events [47]. By culturing cells in the presence of BrdU for two cell cycles, exchanges between differentially stained sister chromatids can be visualized in metaphase spreads. For these experiments, cells were exposed to either SIN-1 or $NO^\bullet/O_2$, cultured in BrdU-containing media for two cell doublings, and analyzed as previously described [40]. As can be seen in Figure 1E, SIN-1 significantly induces SCEs (~6-fold). In addition, although significantly less recombinogenic than SIN-1, $NO^\bullet/O_2$ exposure induces SCEs (~2-fold). Although these results suggest that N_2O_3 induces homologous recombination, it is also possible that $ONOO^-$ that is inevitably formed by reaction of $NO^\bullet$ with intracellular superoxide is responsible for this increase in SCE levels in the $NO^\bullet/O_2$-exposed cells.

Creation of an Interplasmid Recombination Detection Assay

To further explore the relative recombinogenicity of $ONOO^-$- or N_2O_3-induced DNA lesions, we developed an interplasmid recombination assay in which plasmids can be exposed to pure $ONOO^-$ or to conditions that generate exclusively N_2O_3 prior to transfection into the cells. For this purpose, we used plasmids that carry Δ3*egfp* and Δ5*egfp* (Figure 2A). A recombination event between these two plasmids can restore full-length *EGFP*, yielding a fluorescent phenotype. To test the efficacy of this approach, cells were transfected with p*EGFP*, pΔ3*egfp*, or pΔ5*egfp*, or they were cotransfected with both pΔ3*egfp* and pΔ5*egfp*. Whereas ~40% of the cells transfected with the positive control p*EGFP* plasmid were significantly fluorescent, transfection with either pΔ5*egfp* or pΔ3*egfp* alone did not lead

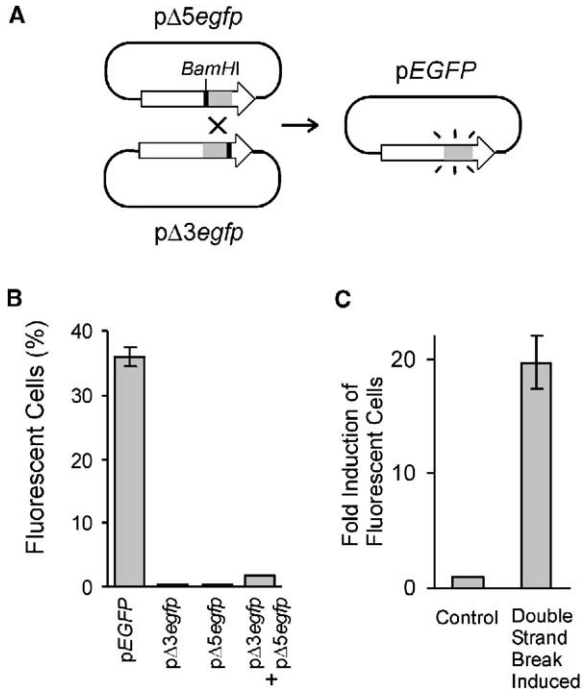

Figure 2. Interplasmid Recombination Assay in Mouse ES Cells and in COS 7L Monkey Kidney Cells

(A) Schematic depicting the interplasmid recombination assay. Expression cassettes are as described in Figure 1B.

(B) Percent fluorescent cells following transfection with the indicated plasmids. ES cells were analyzed by flow cytometry 48 hr after transfection. The p*EGFP* plasmid was used as a positive control.

(C) Double-strand break-induced interplasmid recombination. The pΔ5*egfp* plasmid was linearized at the BamHI site indicated in (A). Fold induction relative to control plasmid (uncut pΔ5*egfp*) is shown.

to any detectable *EGFP* expression (Figure 2B). However, when cells were cotransfected with pΔ5*egfp* and pΔ3*egfp* together, we observed a significant number of fluorescent cells, indicative of interplasmid homologous recombination (related assays have previously been described; e.g., see references [48, 49]).

A time course experiment revealed that the number of fluorescent cells cotransfected with pΔ5*egfp* and pΔ3*egfp* increases over time, reaching a maximal level by ~48 hr, which subsequently begins to decline sometime after 72 hr posttransfection. This rise and fall in the number of fluorescent cells likely reflects the time required to achieve maximal expression of the *EGFP* protein, followed by the inevitable loss of plasmid DNA associated with transient transfections. It is also noteworthy that the cells that carry a single copy of the integrated substrate fluoresce following homologous recombination (which shows that a single copy of an *EGFP* expression cassette is sufficient to yield a detectable fluorescent signal); however, it is not known how many *EGFP* expression cassettes on extrachromosomal DNA are required for such a signal.

In order to use this interplasmid assay to study the relationship between DNA damage and recombination, it is critical to control for transfection efficiency, since cells that receive higher quantities of plasmid have an increased chance of undergoing interplasmid recombination. Under the conditions of these experiments, we found that the transfection efficiency was highly consistent from sample to sample (less than a 10% variation among samples; data not shown). To control for transfection efficiency, the frequencies of interplasmid recombinant cells were normalized according to the percentage of fluorescent cells transfected with the positive control vector (see Experimental Procedures).

Double-strand breaks are known to be potent inducers of homologous recombination, and it has previously been shown that double-strand breaks in plasmids can be repaired by recombining with homologous sequences available on another plasmid [48]. To maximize the sensitivity of the interplasmid assay for detecting damage-induced recombination, we introduced a double-strand break into pΔ5*egfp* using BamHI (Figure 2A) and measured double-strand break-induced recombination under various conditions. Following extensive optimization, we found that we could increase the sensitivity of the assay to damage-induced recombination by an order of magnitude by cotransfecting damaged pΔ5*egfp* with a 10-fold molar excess of pΔ3*egfp* (Figure 2C) and by transfecting cells via lipofection, as opposed to using other transfection methods (data not shown). Given that recombination between two copies of pΔ5*egfp* can never reconstitute full-length *EGFP* coding sequences, conditions in which there is a 10-fold molar excess of pΔ3*egfp* increase the likelihood that recombination events will be detectable by the appearance of a fluorescent signal.

Interplasmid Homologous Recombination Is Induced When Plasmid DNA Is Exposed to $ONOO^-$ and SIN-1, but Not to $NO^•/O_2$

To study the effects of $ONOO^-$-induced DNA lesions, pΔ5*egfp* was exposed to SIN-1 or to purified $ONOO^-$ (see Experimental Procedures). To study the effects of N_2O_3-induced DNA lesions, pΔ5*egfp* was exposed to N_2O_3 in the $NO^•/O_2$ delivery chamber, as described previously [43]. The damaged pΔ5*egfp* was then mixed with undamaged pΔ3*egfp* and transfected into mouse ES cells. Although the frequency of recombination between plasmids could be assessed by quantifying fluorescent cells, if there are too many lesions, then even if there is a productive recombination event, *EGFP* will not be expressed (e.g., due to inhibition of transcription, concurrent mutations, or degradation of damaged plasmid). To determine the optimal dose range, p*EGFP* was exposed to various concentrations of the damaging agents and then transfected into mouse cells, and the proportion of fluorescent cells was assessed. The highest dose at which no significant inhibition of *EGFP* expression was observed was then taken as the upper limit for studies of recombination (Figure 3A). It is noteworthy that even at very high levels of $NO^•/O_2$ exposure, we did not observe any significant inhibition of *EGFP* expression (Figure 3A, right). Therefore, we quantified the number of lesions created under these exposure conditions (described in detail below) and selected an $NO^•/O_2$ dose range that creates a comparable number of lesions per plasmid compared to SIN-1 and

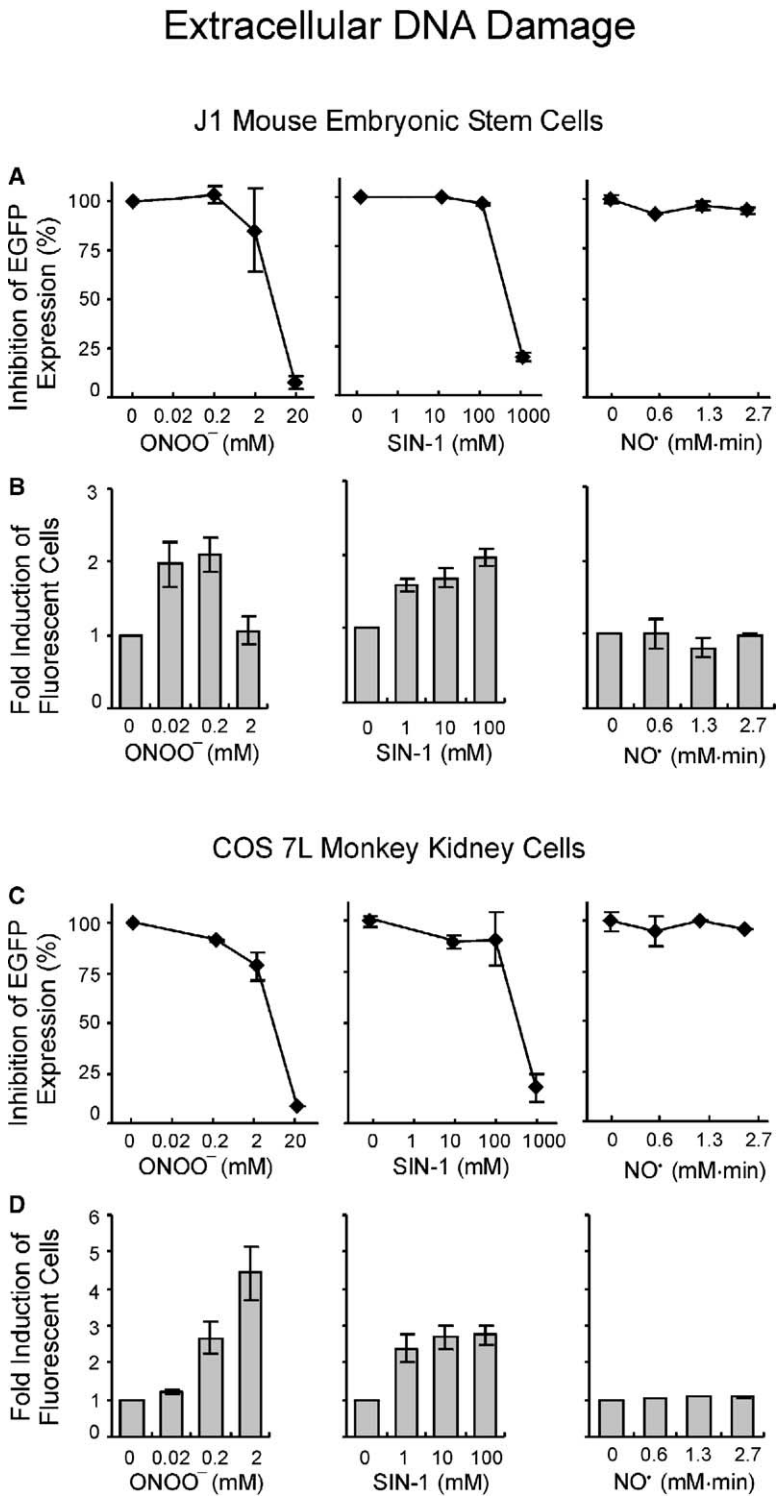

Figure 3. Interplasmid Recombination Induced by ONOO⁻, SIN-1, or $NO^{\bullet}/O_2$-Exposed Plasmid DNA

Results for mouse ES cells (A and B) and in COS 7L monkey kidney cells (C and D) are shown.

(A and C) Inhibition of *EGFP* expression caused by p*EGFP* exposure to ONOO⁻, SIN-1, or $NO^{\bullet}$. The frequency of fluorescent cells was determined by flow cytometry 48 hr after transfection. Values indicate the averages of two independent experiments (± SEM).

(B and D) Interplasmid recombination induced by ONOO⁻, SIN-1, or $NO^{\bullet}/O_2$-exposed pΔ5*egfp*. The pΔ5*egfp* plasmid was exposed to the indicated doses, mixed with undamaged pΔ3*egfp*, and transfected into cells. After 48 hr, the frequency of fluorescent cells was analyzed by flow cytometry. In all the experiments, frequencies were normalized according to the lipofection efficiency. Values indicate two independent experiments, each performed with duplicate samples (± SEM).

ONOO⁻. As can be seen in Figure 3B, DNA lesions induced by ONOO⁻ significantly induced homologous recombination (~2-fold) and DNA exposed to SIN-1 was similarly susceptible to damage-induced recombination. However, DNA lesions created by $NO^{\bullet}/O_2$ exposure did not induce any increase in the frequency of recombination (Figure 3B, right).

Effects of ONOO⁻, SIN-1, and $NO^{\bullet}/O_2$ on Interplasmid Homologous Recombination Are Conserved in Diverse Cell Types

A major advantage to studying damage-induced recombination using extrachromosomal plasmids is that these experiments can be performed in different mammalian cell types. To determine if the observed effects

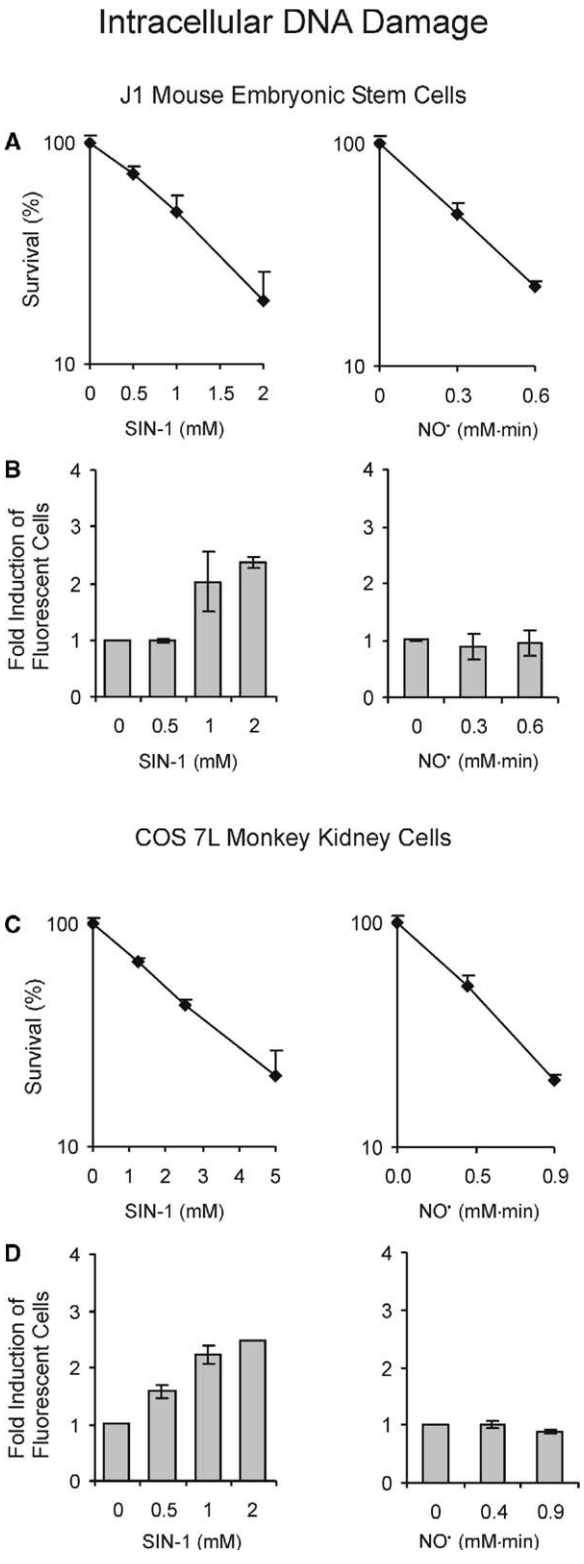

Figure 4. Interplasmid Homologous Recombination Induced by Exposure of Cells to SIN-1 or $NO^{\bullet}/O_2$

Results for mouse ES cells (A and B) and COS 7L monkey kidney cells (C and D) are shown.

(A and C) Relative toxicity induced by exposure to the indicated doses of $NO^{\bullet}$ or SIN-1 as determined by colony forming assays. For $NO^{\bullet}/O_2$ exposure, Ar gas was used as a negative control, and relative survival was normalized accordingly. Values are the mean of three samples ± SEM.

(B and D) Interplasmid recombination induced by SIN-1 or $NO^{\bullet}/O_2$ in cells that carry pΔ5*egfp* and pΔ3*egfp*. Cells were colipofected with pΔ5*egfp* and pΔ3*egfp* 24 hr prior to exposure to the indicated doses of SIN-1 or $NO^{\bullet}$. After 48 hr, the frequency of fluorescent cells was quantified by flow cytometry. In all the experiments, frequencies were normalized according to the lipofection efficiency. Values indicate two independent experiments, each performed with duplicate samples (± SEM).

of $ONOO^-$, SIN-1, and $NO^{\bullet}/O_2$ on interplasmid homologous recombination are similar in other mammalian cell types, we repeated these experiments using COS-7L African green monkey kidney cells. Despite the fact that these are very different cell types from two different species, we saw remarkably similar dose-response curves when we assayed for inhibition of *EGFP* expression (Figure 3C). Furthermore, although there are differences in the responses of these two cell types to damage-induced recombination (e.g., the minimal dose required to induce recombination), overall the relative recombinogenicity of these exposures is highly similar (Figure 3D).

Exposure of Mammalian Cells to $ONOO^-$ and SIN-1, but Not to $NO^{\bullet}/O_2$, Induces Extrachromosomal Recombination

One of the strengths of the interplasmid recombination assay is that by damaging the plasmid prior to transfection into cells, the effects of specific DNA lesions can be studied. Another advantage of this assay is that it can be readily adapted to many different cell types. Finally, in addition to introducing damage to the plasmids prior to transfection, the cells can also be exposed to damaging agents posttransfection to explore the possibility that concurrent cellular responses to damage exposure significantly modify the effects of DNA lesions on recombination.

We have shown above that the relative recombinogenicity of DNA lesions created by $ONOO^-$ and SIN-1 versus $NO^{\bullet}/O_2$ are similar in both mouse ES and monkey COS 7L cells (Figure 3). We next asked if different cell types would respond similarly when the cells themselves, rather than plasmid DNA, are exposed to SIN-1 and $NO^{\bullet}/O_2$. To select the appropriate dose range, we first established the dose-dependent survival of COS 7L cells to SIN-1 or $NO^{\bullet}/O_2$ (Figure 4C; note that Figure 4A is the same as Figure 1C and is included here for ease of comparisons). COS 7L cells appear to be more resistant to the toxic effects of both SIN-1 and $NO^{\bullet}$ when compared to mouse ES cells (compare Figures 4A and 4C; note the change in the dose range).

To study interplasmid recombination in exposed cells, we cotransfected cells with undamaged pΔ5*egfp* and pΔ3*egfp* and after 24 hr (to allow time for recovery from transfection), we exposed the cells to increasing concentrations of SIN-1 or to $NO^{\bullet}/O_2$. After an additional 48 hr, the cells were analyzed by flow cytometry (note that similar results were observed in pilot experiments assayed either 48 or 72 hr post damage exposure). For both ES and COS 7L cells, exposure to SIN-1 after transfection caused a dose-dependent induction

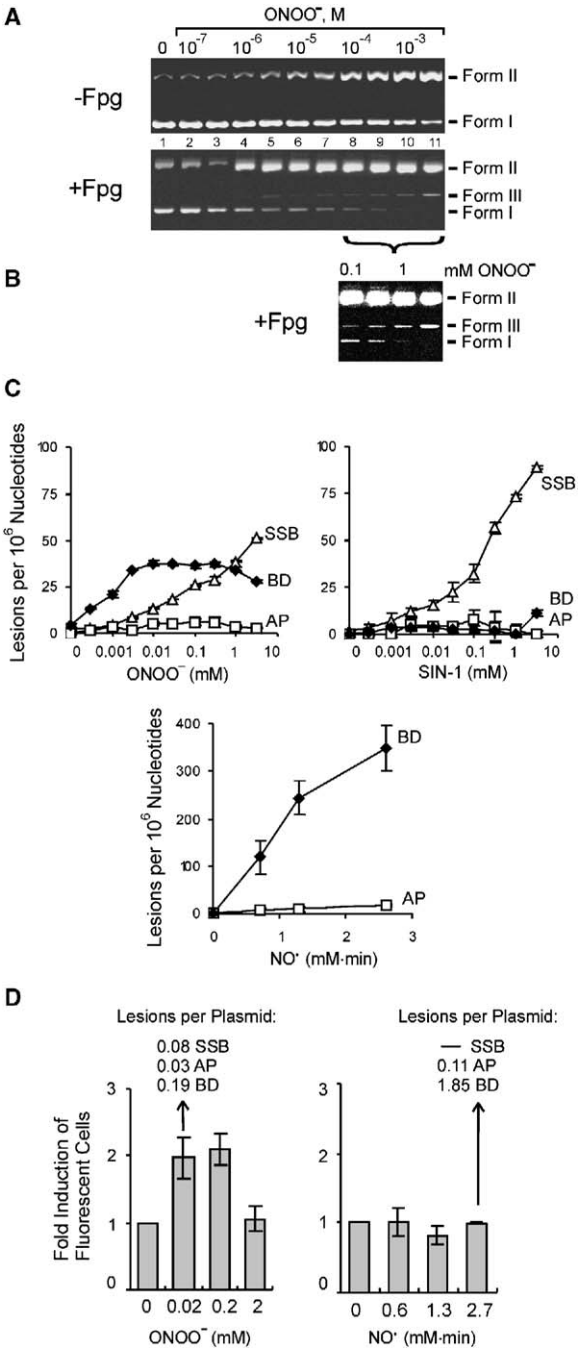

Figure 5. Quantification of the Major Classes of DNA Lesions Induced by ONOO⁻, SIN-1, and NO•/O_2 In Vitro and Comparison of Lesion Levels to Recombination Levels

(A) Example of gel electrophoretic analysis in the plasmid nicking assay used to quantify base and deoxyribose lesions. For technical reasons, the plasmid nicking assays were performed with pSP189; this plasmid is similar in size to p∆5*egfp* (both are ~5 kb). Upper panel: direct single-strand breaks produced in plasmid pSP189 by ONOO⁻ cause a dose-dependent shift from form I (supercoiled) to form II (nicked, closed-circular plasmid). Lower panel: ONOO⁻-treated plasmid DNA was reacted with Fpg to convert base lesions and abasic sites to strand breaks. Fpg incubation causes the appearance of linear plasmid (form III). ONOO⁻ concentrations are in half-log steps.

(B) The brightness and contrast of lanes 8–11 in the bottom panel of (A) were adjusted to emphasize the appearance of form III DNA.

(C) Quantity of base damage (BD), abasic sites (AP), and single-strand breaks (SSB) per 10^6 nucleotides as determined by plasmid topoisomer analysis. Levels of base adducts were estimated by converting base lesions to single-strand breaks using purified Fpg glycosylase for ONOO⁻ and SIN-1, or purified Ung and AlkA glycosylases followed by putrescine cleavage of abasic sites for NO•/O_2. Mean ± SD for n = 4. Note that the base damage data for SIN-1 and ONOO⁻ has been previously reported [72].

(D) A comparison of the quality and quantity of lesions created by the lowest recombinogenic dose of ONOO⁻ and the highest dose of NO•/O_2. Graphs are identical to those in Figure 3B and are shown here to facilitate comparison to damage levels.

of recombination (Figures 4B and 4D). Importantly, the same dose of SIN-1 resulted in a similar fold induction in both cell types. For example, exposure to 1 mM SIN-1 induces an ~2 fold increase in the frequency of recombination in both cell types, regardless of whether the exposure occurred before or after transfection (Figures 3B–3D). Therefore, it does not appear that cellular responses to damage exposure dramatically alter the magnitude of SIN-1-induced interplasmid homologous recombination (despite the differences in toxicity in these cell types at the selected doses). Consistent with the previous analysis of recombination between p∆5*egfp* and p∆3*egfp* (e.g., Figures 1D and 3), we did not observe any significant induction of recombination when cells were exposed to NO•/O_2. Thus, it again appears that DNA lesions induced by ONOO⁻ are significantly more recombinogenic than those induced by NO•/O_2.

ONOO⁻-Induced Direct Single-Strand Breaks and Oxidative Base Lesions Are Recombinogenic

Reactive nitrogen species produce three major classes of lesions: base damage, abasic sites, and single-strand breaks. To gain a better understanding of how these different classes of lesions affect homologous recombination, we used a well-established plasmid nicking assay to quantify lesions generated when plasmid is exposed to ONOO⁻, SIN-1, or N_2O_3 [24, 33]. Topoisomer analysis was performed to quantify single-strand breaks (by direct analysis of damaged plasmids), abasic sites (which were converted to strand breaks using putrescine), and base lesions (which were converted to strand breaks using a combination of purified DNA glycosylases and putrescine). The relative proportions of supercoiled, relaxed, and linear plasmid molecules were then used to calculate the number of DNA lesions (see Experimental Procedures).

An example of an experiment in which the frequency of Fpg-sensitive lesions was estimated is shown in Figure 5A. In the absence of Fpg, with increasing doses of ONOO⁻, there is a gradual shift from form I (supercoiled DNA) to form II (nicked closed-circular DNA), which reflects the ability of ONOO⁻ to directly induce single-strand breaks. Plasmid was then digested with purified Fpg glycosylase, which both removes damaged bases and cleaves the backbone via its associated lyase activity [36]. In the case of control undamaged plasmid DNA that was analyzed before and after incubation with Fpg glycosylase (Figure 5A, lane 1), there is very little

change in the ratio of supercoiled (form I) and nicked (form II) plasmid following digestion with Fpg (Fpg produced a small amount of the plasmid nicking, most likely as a consequence of cutting at background damage). In contrast, at the highest concentration of $ONOO^-$ (5 mM, far right lane), digestion with Fpg eliminates nearly all of the supercoiled form I DNA, indicating that essentially all of the plasmids had at least one Fpg sensitive site. Importantly, it also appears that Fpg induces a small but detectable level of double-strand breaks, as indicated by the appearance of linear form III DNA, made more apparent by the adjustment in contrast shown in Figure 5B.

The ratio of forms I and II can be used to estimate the number of lesions per million nucleotides (although the total amount of DNA per lane can vary depending on loading, the ratio remains constant). Using this topoisomer approach, we estimated the levels of chemically induced single-strand breaks, abasic sites, and base lesions. The distinction between guanine oxidation products arising from $ONOO^-$ [50] and the nucleobase deamination products arising from N_2O_3 [24] was achieved by differential recognition of the lesions by Fpg and Ung/AlkA, respectively (see Experimental Procedures). We found that $ONOO^-$ creates primarily base damage and single-strand breaks, whereas SIN-1 creates primarily single-strand breaks (Figure 5C). In contrast, $NO^\bullet/O_2$ exposure creates almost exclusively base lesions, with a small number of abasic sites and an undetectable level of single-strand breaks, (Figure 5C), which is consistent with our published studies of the N_2O_3-induced DNA damage spectrum [24]. It is noteworthy that base lesions and abasic sites are masked by the presence of single-strand breaks in the topoisomer assay. Thus, above 60 lesions per million nucleotides, there is more than one damage event per plasmid molecule on average (according to a Poisson distribution), so that the calculated levels of damage underestimate the true level of damage (this is likely the reason for the appearance of a plateau in base damage levels with doses of $ONOO^-$ above 0.01 mM; Figure 5C). This behavior is independent of the identity of the DNA damaging agent, however, so corrective measures are not necessary when making comparisons of different agents, as in the present studies.

In order to gain a better understanding of the classes of lesions that lead to recombination, we compared the quantity and quality of lesions created by the lowest recombinogenic dose of $ONOO^-$ (0.02 mM) to those created by the highest dose of $NO^\bullet$ (2.7 mM·min) used for the interplasmid recombination assay. Although 2.7 mM·min $NO^\bullet$ creates more abasic sites and many more base lesions than 0.02 mM $ONOO^-$ (Figure 5D), $NO^\bullet$ was not recombinogenic whereas $ONOO^-$ was highly recombinogenic. Importantly, $NO^\bullet$ does not create any detectable single-strand breaks, whereas significant levels of single-strand breaks were detected at recombinogenic doses of $ONOO^-$. Note that the masking effect of single-strand breaks likely results in only a minor underestimate of the number of base lesions at 0.02 mM $ONOO^-$, so on a per lesion basis, $ONOO^-$ is more recombinogenic than $NO^\bullet$. We therefore conclude that single-strand breaks induced by deoxyribose oxidation and oxidatively damaged bases are significantly more recombinogenic than nucleobase deamination products in mammalian cells.

It is well established that double-strand breaks induce homologous recombination in mammalian cells [51, 52]. Although DNA exposed to 0.2 mM $ONOO^-$ was highly recombinogenic, none of the plasmid DNA appeared to have been linearized by exposure to 0.2 mM $ONOO^-$ (this dose falls between lanes 8 and 9 in the top gel in Figure 5A). However, following digestion with Fpg in vitro, double-strand breaks can be detected by the appearance of linear DNA (see lanes 8 and 9 in the lower gel of Figure 5A, and in Figure 5B). In contrast to $ONOO^-$, digestion of $NO^\bullet/O_2$-treated DNA with glycosylases did not yield any detectable linear DNA (data not shown). Intriguingly, at 1–5 mM $ONOO^-$, digestion with Fpg essentially eliminates the supercoiled form I DNA, and it is around this dose range that the frequency of induced recombination appears to decline (compare 0.2 and 2 mM $ONOO^-$ in Figure 5D, left) and the percentage of cells able to express *EGFP* from the $ONOO^-$-treated positive control pEGFP vector starts to plummet (Figures 3A and 3C). When DNA is transfected by microinjection into mammalian cells, most of the DNA is rapidly degraded by cytosolic nucleases [53]. Furthermore, it has been shown that whereas supercoiled plasmid yields high levels of expression from a marker transgene 72 hr post lipofection, linearized DNA yields no detectable expression [54]. Given that mammalian cells harbor multiple DNA glycosylases that act on a broad range of substrates [36, 55], it is likely that a much greater proportion of the damaged plasmid is linearized by mammalian glycosylases following transfection than by Fpg digestion in vitro, rendering the DNA vulnerable to nucleolytic degradation. Taken together, these results suggest that following transfection, mammalian DNA glycosylases create double-strand breaks that both induce homologous recombination and render the DNA vulnerable to degradation by exonucleases.

Discussion

It has long been known that chronic inflammation contributes to cancer. Although it is well established that $NO^\bullet$ creates reactive nitrogen species that form mutagenic DNA lesions [9, 10, 35], very few studies had investigated the possibility that $NO^\bullet$ induces homologous recombination events, even though homologous recombination causes sequence rearrangements that are known to contribute to cancer [16, 18, 56]. Indeed, dozens of known carcinogens are recombinogens [17, 19]. Furthermore, people who are born predisposed to spontaneously high levels of recombination are prone to cancer [18, 19]. Thus, whether caused by exposure or by an inherited predisposition, homologous recombination events are a form of genetic instability that can contribute to cancer.

Here, we have shown that $ONOO^-$, the product of the reaction of $NO^\bullet$ with superoxide, causes highly recombinogenic DNA lesions. In contrast, when $NO^\bullet$ reacts with oxygen to form N_2O_3, the resulting DNA lesions did not induce a detectable increase in interplasmid recombination. Therefore, $NO^\bullet$ becomes particularly recombi-

nogenic specifically under conditions where it reacts with superoxide to create $ONOO^-$. Importantly, $NO^\bullet$ mediates both cell signaling and inflammation, but only under conditions of inflammation does the body simultaneously create high levels of both $NO^\bullet$ and superoxide. Therefore, it is likely that $NO^\bullet$ does not significantly induce recombination when produced at low concentrations during cell-signaling, whereas the results of the present studies show that following reaction with superoxide, it becomes highly recombinogenic and can thus contribute to tumorigenic sequence rearrangements.

We are primarily interested in the effects of inflammatory chemicals on genomic stability under physiologically relevant exposure conditions. In the case of $NO^\bullet/O_2$, it has been estimated that the steady-state concentration of $NO^\bullet$ at sites of inflammation is ≤ 1 μM [4, 57, 58]. In the studies described here, cells were exposed to 1.3 μM $NO^\bullet$ (steady state), which is a reasonable approximation of the level expected to be present within inflamed tissues. In terms of $ONOO^-$, we elected not to expose cells to pure $ONOO^-$, because if added to the media, the result would be a bolus exposure that does not accurately reflect conditions during inflammation (the half-life of $ONOO^-$ is ~50 ms [59]). In contrast to $ONOO^-$, SIN-1 makes it possible to achieve longer term exposures, since SIN-1 decomposes to form $ONOO^-$ at a fairly steady rate (at least during the first 90 min of exposure [60]). At 1 mM SIN-1, $ONOO^-$ is produced at a rate of ~0.2 μM/s [60], and in the studies presented here, 0.5 mM SIN-1 significantly induced homologous recombination at the integrated direct repeat substrate (note that this exposure was also relatively nontoxic; see Figures 1C–1D). Although the exact concentrations of $ONOO^-$ at sites of inflammation are not yet known, the conditions used in these experiments are on par with the expected nanomolar to micromolar range of $ONOO^-$ concentrations thought to be present during inflammation [4].

Comparisons of $ONOO^-$-induced recombination (reported here) and $ONOO^-$-induced mutations (reported in the literature) suggest that $ONOO^-$ is similarly potent as both a mutagen and a recombinogen. For example, at a dose of SIN-1 that kills ~75% of TK6 cells, mutations at HPRT and TK are induced by ~2-fold [23, 61], whereas in the studies presented here, a dose of SIN-1 that kills ~25% of the cells induced a ~3-fold increase in recombination at a single locus in the chromosomally integrated recombination substrate. These results suggest that $ONOO^-$ may be as recombinogenic as it is mutagenic, although further studies are required, since toxicity does not necessarily directly reflect the levels of damage. Comparing the studies presented here to those in which exposed plasmid DNA has been used to study mutagenesis (thus avoiding the complexities of assessing damage levels in cells), we again found similarities in the mutagenic and recombinogenic effects of $ONOO^-$. Specifically, in previous studies using extrachromosomal plasmids, 2–2.5 mM $ONOO^-$ induced a 4- to 9-fold increase in point mutations, respectively [9, 33]. Here, we found that 0.02 mM $ONOO^-$ induced a 2-fold increase in interplasmid recombination in mouse ES cells, and that 2 mM $ONOO^-$ induced a 4-fold increase in interplasmid recombination in monkey kidney cells. Although further studies are necessary to control for cell-type effects, these comparisons suggest that the mutagenic potential of $ONOO^-$ is on par with its recombinogenic potential.

Although double-strand breaks are thought to be critical for inducing homologous recombination, $ONOO^-$ creates oxidative base lesions, abasic sites, and single-strand breaks [4]. Consistent with previous studies, in the topoisomer analysis performed here, we were unable to detect the presence of any $ONOO^-$- or SIN-1-induced double-strand breaks at doses that were highly recombinogenic. However, we have shown that Fpg can introduce double-strand breaks in $ONOO^-$-treated plasmids (Figure 5A) and in SIN-1-treated plasmids (data not shown). In contrast, treatment with DNA glycosylases did not induce double-strand breaks in $NO^\bullet/O_2$-treated plasmids (data not shown). Thus, following transfection, closely opposed lesions on opposite strands could potentially be converted into double-strand breaks by DNA glycosylases, as was originally shown for oxidative damage in vitro and has been recently demonstrated for radiation damage in mammalian cells [37, 38, 42]. Alternatively, abasic sites and single-strand breaks may be converted into double-strand breaks during replication, which is likely to contribute to SIN-1-induced recombination at the integrated direct repeat. However, given that the plasmids used in these experiments do not have an origin of replication, the most likely cause of interplasmid recombination induced by $ONOO^-$ are double-strand breaks created by enzymatic processing in the recipient cells.

The results of these studies show that conditions that favored formation of N_2O_3 did not induce recombination at any of the recombination substrates, although there was a small but significant increase in sister chromatid exchanges in cells exposed to $NO^\bullet/O_2$. It is certainly possible that some of the lesions induced by N_2O_3 induce SCEs that were not detected using the engineered substrates. However, due to the inevitable presence of superoxide in normal cells, it is also possible that $NO^\bullet$ reacts with superoxide to form ONOO in these cells. Nevertheless, it is clearly the case that $ONOO^-$ is significantly more recombinogenic than N_2O_3 in all of the recombination assays, and N_2O_3 lesions failed to induce any detectable increase in interplasmid recombination. These results were somewhat unexpected, given that lesions created by both N_2O_3 and $ONOO^-$ are substrates for the base excision repair pathway, and that base excision repair intermediates have been shown to be highly recombinogenic in mammalian cells (e.g., [39, 40]).

One major difference between $ONOO^-$ and N_2O_3 is that $ONOO^-$ can directly react with deoxyribose to induce single-strand breaks. Therefore, it is possible that chemically induced single-strand breaks are converted into recombinogenic double-strand breaks when another single-strand break is enzymatically introduced on the opposite strand by base excision repair enzyme(s). Given that glycosylases rapidly find their targets ($t_{1/2}$ = minutes for the Aag DNA glycosylase, for example [62]), it is not difficult to imagine that a glycosylase might find its target before a chemically induced strand break on the opposite strand has been repaired. Furthermore, different types of glycosylases act on

$ONOO^-$-induced guanine oxidation and nitration products (e.g., 8-nitroguanine, 8-oxoguanine and its secondary oxidative products) compared to N_2O_3-induced nucleobase deamination products (uracil, xanthine, and hypoxanthine [50, 63]; M.D. et al., in preparation). The vast majority of $ONOO^-$-induced lesions are repaired by bifunctional glycosylases (Fpg and Nth, and their mammalian homologs), and these enzymes have the ability both to remove the base lesions and to cleave the sugar-phosphate backbone (i.e., via their associated lyase activity) [64, 65]. In contrast, those glycosylases known to act on N_2O_3-induced lesions are monofunctional (e.g., Ung and AlkA, and their mammalian homologs [63, 66]; M.D. et al., unpublished data), so these enzymes remove the base lesions but cannot create single-strand breaks. Taken together, the observation that $ONOO^-$ is more recombinogenic than N_2O_3 may be because bifunctional glycosylases can create recombinogenic double-strand breaks by cleaving across from a pre-existing chemically-induced strand break and by enzymatic cleavage at two closely opposed base lesions.

Although deaminated bases are known to be mutagenic [27], we did not find that *EGFP* expression was inhibited by exposure to $NO^\bullet/O_2$. At the highest dose of $NO^\bullet/O_2$, we estimated that there are ~2 lesions/plasmid. Given that only ~15% of the plasmid sequences code for *EGFP*, it is likely that copies of the plasmid that harbor undamaged coding sequences are responsible for the observed *EGFP* expression. Unexpectedly, we found that an even lower number of $ONOO^-$ lesions/plasmid inhibited *EGFP* expression. Following the same logic, it seems unlikely that *EGFP* expression is suppressed by mutagenic damage to coding sequences. Given that linearized plasmid DNA is highly vulnerable to degradation by exonucleases [53, 54], one possibility is that *EGFP* expression is suppressed due to plasmid loss, rather than to mutations. Thus, the observations that suppression of *EGFP* and induction of recombination go hand in hand for $ONOO^-$ and SIN-1, and that $NO^\bullet/O_2$ neither suppresses *EGFP* nor induces recombination, are consistent with a model wherein glycosylases introduce double-strand breaks that both increase the vulnerability of the DNA to degradation and induce homologous recombination.

One interesting result of these studies was that the relative recombinogenicity of $ONOO^-$ and N_2O_3 is very similar in mouse embryonic cells and monkey kidney cells, regardless of whether the DNA was exposed prior to transfection, or cells were exposed after transfection. However, there are also some subtle differences. For example, there is a significant difference in the doses of $ONOO^-$ required to achieve maximal induction of recombination in embryonic cells versus kidney cells (Figure 3). Although there are many possible explanations for this observation, one possibility is that embryonic stem cells have relatively higher levels of DNA glycosylase that induce double-strand breaks. If this were the case, then glycosylase-induced double-strand breaks could potentially be induced at lower levels of adducts. Although $ONOO^-$-induced recombination is a general feature of mammalian cells, these results show that the relative sensitivity of cells to $ONOO^-$-induced recombination clearly is variable among different cell types.

The magnitude of $ONOO^-$-induced recombination is significant. Mammalian cells subjected to conditions that favor formation of $ONOO^-$ are susceptible to an ~3-fold increase in recombination at the integrated ΔGF recombination substrate, and to an ~6-fold increase in SCEs. For comparison, it has been reported that phenytoin, an oxidizing agent, induces a 2- to 3-fold increase in recombination at an analogous direct repeat substrate in CHO cells [67]. Indeed, in the SCE literature, most of the agents that induce such high levels of SCEs are chemicals that most of us will never experience [68]. Given that inflammation is unavoidable in the lifetime of most people, and that $ONOO^-$ is highly recombinogenic, endogenously produced $ONOO^-$ may be one of the most significant recombinogens to which most people are exposed. As such, $ONOO^-$-induced recombination may be an important risk factor for tumorigenesis.

Significance

Homologous recombination events are an important class of mutations that are likely to be the underlying cause of one or more mutations in every tumor. Nevertheless, we do not yet know what causes recombination in people. Although exposure to toxic levels of most carcinogens is recombinogenic, most humans are not likely to be exposed to high concentrations of these agents. In contrast, inflammation is a widespread pathophysiological response in humans, and it is known to contribute to cancer. Indeed, during inflammation, the high levels of reactive oxygen and nitrogen species that are produced by activated macrophages are highly toxic to neighboring normal cells. The major physiologically relevant reactive nitrogen species are N_2O_3 and $ONOO^-$, which are formed when $NO^\bullet$ reacts with either oxygen or superoxide, respectively. Here, we have shown that $ONOO^-$ is a strong recombinogen, whereas N_2O_3 is relatively weakly recombinogenic. Consequently, $NO^\bullet$ becomes highly recombinogenic specifically under conditions when superoxide is present, as is the case during inflammation. Measurements of $ONOO^-$-induced sister chromatid exchange, recombination at a chromosomally integrated direct repeat, and interplasmid recombination definitively show that $ONOO^-$-induced lesions are highly recombinogenic. Taken together, these results suggest that $ONOO^-$-induced recombinogenic DNA damage may play an important role in inflammation-induced cancers.

Experimental Procedures

Cell Culture

Mouse embryonic stem cells (J1) were maintained in DMEM containing 10% fetal bovine serum, L-glutamine, nonessential amino acids, β-mercaptoethanol, and leukocyte inhibitory factor on gelatinized dishes without feeders. The COS-7L African green monkey kidney cell line (Invitrogen) was maintained in DMEM containing 10% fetal bovine serum and L-glutamine.

ΔGF Cells

Embryonic stem cells were engineered to carry a direct repeat recombination substrate integrated at the ROSA26 locus. The design of this substrate is similar to that of the FYDR substrate [46], ex-

cept that reconstitution of full-length coding sequences leads to expression of enhanced green fluorescent protein (rather than yellow fluorescent protein). This recombination detection system will be more fully described elsewhere [44].

SIN-1 Treatment of Cells

Cells were plated in complete medium 24 hr prior to treatment. Cells were exposed to the indicated doses of SIN-1 (Biomol Research Laboratories) in Dulbecco's PBS supplemented with 25 mM sodium bicarbonate (pH 7.4), at 37°C. Exposure of cultures to air was provided by shaking for 5 min every 10 min for 90 min, as described previously [61]. After treatment, cultures were rinsed in PBS and incubated in fresh medium.

NO• Treatment of Cells

Cells were plated at a density of 0.5–2 × 10^6 cells per 60 mm dishes in complete medium. After 24 hr, log phase cells were exposed to 10% NO•/90% Ar gas mixture (BOC Gas Co.) which was passed through 7 cm of Silastic tubing in the NO• delivery chamber, as previously described [43]. A 50% O_2/45% N_2/5% CO_2 gas mixture (BOC Gas Co.) was passed through a second 7 cm long tube to maintain the O_2 level in the medium. These conditions produced steady-state levels of O_2 and NO• that are approximately those that are experienced under physiological conditions (NO• steady-state levels in these experiments are 1.84 μM; physiological levels are on the order of ~1 μM) [4, 57, 58]. The control cells were exposed to 100% Ar gas under the same conditions as NO• exposure. At the end of treatment, cells were washed and incubated in fresh complete medium.

Colony Forming Assay

Following treatment with SIN-1 and NO•/O_2, cells were harvested by trypsinization, counted, and plated at a density of 100 cells/100 mm tissue culture dishes. After a week of culture, the colonies were fixed with ethanol, stained with trypan blue, and counted. Experiments were performed in triplicate and all experiments were performed three or more times.

SCE Assay

J1 cells were seeded at a density of 1 × 10^6 per 100 mm dish for SIN-1 treatments, and at 0.5 × 10^6 per 60 mm dish for NO•/O_2 treatment. After 24 hr, log phase cultures were exposed to SIN-1 and NO•/O_2 as described above. After exposure, cells were washed and incubated in fresh McCoy's 5A media (Invitrogen) supplemented with 10 μM BrdU. After 24 hr, Colcemid (0.1 μg/ml; Invitrogen) was added to the medium for an additional 3 hr. Metaphase spreads were prepared, and sister chromatids were differentially stained as previously described [40]. Experiments were performed in duplicate, and 20 metaphase spreads were counted per data point.

Chromosomal Direct Repeat Assay

Between 0.5 and 2.5 × 10^5 ΔGF cells were seeded onto six-well dishes for SIN-1 treatments, and onto 60 mm tissue dishes for NO•/O_2 treatment. After 24 hr, log phase cells were exposed to the indicated doses of cytotoxic agents, as described above. After 72 hr (~3.25 population doublings in control cells), cells were harvested by trypsinization and analyzed by flow cytometry to determine the frequency of fluorescent cells.

Plasmid Construction to Generate Recombination Substrates

The PstI-BamHI fragment in pCX-*EGFP* (gift of M. Okabe [69]) was replaced with a synthetic adaptor carrying NsiI, NotI, and XhoI sites to create pCX-NNX-*EGFP*. Full-length and truncated coding sequences were PCR amplified using primers that carry synthetic ApoI sites and subcloned between the EcoRI sites of pCX-NNX to create pCX-NNX-Δ5*egfp* (abbreviated as pΔ5*egfp*) and pCX-NNX-D3*egfp* (abbreviated as pΔ3*egfp*). The pΔ5*egfp* plasmid carries a 99 bp deletion from the 5′ end, and pΔ3*egfp* carried an 81 bp deletion from the 3′ end of the open reading frame. There are 540 bp of overlap between the deletions. Stop codons were placed after and before these cassettes, respectively, to prevent read-through translation products. Plasmid DNA was purified using the Qiagen plasmid purification kit. Restriction enzymes were from New England Biolabs. Oligonucleotides were from Amitof, Inc. (Allston, MA). Oligonucleotide and plasmid sequences are available upon request.

ONOO⁻, SIN-1, and NO• Treatment of Plasmid DNA

ONOO⁻ was synthesized by ozonolysis of sodium azide [70], and the concentration of the stock solution was measured by UV immediately prior to treatment (ϵ_{302} = 1670 M^{-1} cm^{-1}). Bolus exposure to ONOO⁻ was achieved by placing a droplet of the ONOO⁻ stock solution on the side wall of a microcentrifuge tube containing plasmid DNA (2.5 μg in 50 μl) in 150 mM potassium phosphate/20 mM sodium bicarbonate buffer (pH 7.4) followed by vigorous vortexing to mix the solutions. For SIN-1, plasmid DNA (5 μg in 100 μl) was treated in 150 mM potassium phosphate/20 mM sodium bicarbonate buffer (pH 7.4) at 37°C for 90 min. For NO• treatment, plasmid DNA (20 μg/ml) was exposed in the NO• delivery chamber under the same conditions as used for the cell exposures (see above). The NO• dose was controlled by removing samples at various times during exposure. For all treatments, after exposure, the DNA was recovered by ethanol precipitation, resuspended in PBS, and quantified by UV spectrometry.

Interplasmid Recombination Assay

Extracellular DNA Exposure

J1 and COS-7L cells were plated at a density of 4 × 10^4 cells per well in 24-well plates. After 24 hr, 0.1 μg pΔ5*egfp* (± exposure to DNA damage) and 1 μg pΔ3*egfp* plasmids were colipofected into the cells by using Lipofectamine 2000 (Invitrogen) in a total volume of 0.5 ml. To assay inhibition of *EGFP* expression, 0.1 μg of p*EGFP* was treated with the indicated doses of these agents prior to lipofection. Transfection efficiency in each experiment was measured by simultaneous lipofection of 0.1 μg p*EGFP* in three independent samples. To keep DNA concentrations constant, 0.1 μg of damaged pLacZ (Clontech) was used in lieu of damaged pΔ5*egfp*, and 1 μg of pLacZ was used in lieu of pΔ3*egfp*. For all experiments, cells were trypsinized 48 hr post-lipofection and analyzed by flow cytometry to determine the frequency of fluorescent cells.

Intracellular DNA Exposure

J1 and COS-7L cells were plated at a density of 4 × 10^4 cells per well in six-well plates. After 24 hr, 0.3 μg pΔ5*egfp* and 0.3 μg pΔ3*egfp* plasmids were colipofected into the cells in a total volume of 1 ml as described above. After 24 hr, cells were treated with SIN-1 or NO•/O_2 as described above. Cells were analyzed by flow cytometry 48 hr posttreatment. The transfection efficiency was tested by simultaneous lipofection of 0.3 μg p*EGFP* into three independent samples.

Flow Cytometry

Pelleted cells were resuspended in OptiMEM (GIBCO/BRL) and passed through a 70 μm filter (Falcon) prior to analysis on a Becton Dickinson FACScan flow cytometer (excitation 488 nm, argon laser; emission 580/30). Live cells were gated according to forward and side scatter.

Quantification of DNA Damage by Plasmid Topoisomer Analysis

A plasmid nicking assay was used to quantify the DNA deoxyribose and base damage. For lesion quantification, similar results were obtained using either the pΔ5*egfp* or the plasmid pSP189. The latter is a pBR-based, 4952 bp plasmid, which is similar in size to pΔ5*egfp* (4921 bp), which allows interchangeability of the two plasmids in the nicking assay. After ONOO⁻, SIN-1, or NO•/O_2 treatments, a portion (200 ng) of the DNA was treated with putrescine (100 mM [pH 7.0], 1 hr, 37°C) to convert all types of abasic sites to strand breaks [51, 71]. Another portion (200 ng) was kept on ice as a control for the direct strand breaks. To quantify the oxidative base lesions formed by ONOO⁻ or SIN-1, a third portion of the DNA sample was treated with *E. coli* formamidopyrimidine-DNA glycosylase (Fpg) (Trevigen) to convert oxidized purines to strand breaks. More than 90% of the ONOO⁻ guanine oxidation products in DNA are recognized by Fpg [50]. Fpg treatment was performed in a volume of 10 μl containing 200 ng of ONOO⁻-treated DNA, 1 μl of Fpg

(~1.5 units) and buffer containing 10 mM Tris-HCl (pH 7.5), 1 mM EDTA, and 100 mM NaCl at 37°C for 1 hr. Fpg was then removed by phenol/chloroform extraction. Similarly, to quantify nucleobase deamination products formed by $NO^{\bullet}$ in the presence of O_2 (e.g., N_2O_3), plasmid DNA samples were incubated with *E. coli* Ung DNA glycosylase (Trevigen) and the *E. coli* AlkA DNA glycosylase (Pharmingen), followed by putrescine treatment to convert the resulting abasic sites to strand breaks. Both xanthine and hypoxanthine have been shown to be recognized by AlkA ([63]; M.D. et al., unpublished data). Crossreactions of AlkA/Ung with $ONOO^-$-treated DNA and Fpg with N_2O_3-treated DNA revealed <5% additional strand breaks, which demonstrates the specificity of these enzymes for the specific sets of lesions caused by N_2O_3 and $ONOO^-$. The recovered DNA was redissolved in H_2O, and plasmid topoisomers were resolved by 1% agarose slab gel electrophoresis in the presence of 0.1 μg/ml ethidium bromide. The quantity of DNA in each band was determined by fluorescence imaging (Ultra-Lum). For lesion quantification, similar results were obtained using either the pΔ5*egfp* or the pSP189 plasmid (provided by Dr. M. Seidman; NIH, Bethesda, MD), with the pSP189 plasmid used for the experiments presented in Figure 5. Note that the base damage data for SIN-1 and $ONOO^-$ has been previously reported [72].

Acknowledgments

We are grateful to T. Matsuguchi and E.J. Spek for creating the plasmids used in the interplasmid recombination assay. We thank the Center for Cancer Research Flow Cytometry Facility. We thank L.J. Trudel for assistance in $NO^{\bullet}$ exposures. Research is supported by R01CA79827 (B.P.E.), P01-CA26735 (B.P.E. and P.C.D.), and the Center for Environmental Health Sciences (ES02109).

Received: September 20, 2004
Revised: December 20, 2004
Accepted: December 21, 2004
Published: March 25, 2005

References

1. Moncada, S., and Higgs, E.A. (1991). Endogenous nitric oxide: physiology, pathology and clinical relevance. Eur. J. Clin. Invest. *21*, 361–374.
2. Kerwin, J.F., Jr., Lancaster, J.R., Jr., and Feldman, P.L. (1995). Nitric oxide: a new paradigm for second messengers. J. Med. Chem. *38*, 4343–4362.
3. Wiseman, H., and Halliwell, B. (1996). Damage to DNA by reactive oxygen and nitrogen species: role in inflammatory disease and progression to cancer. Biochem. J. *313*, 17–29.
4. Dedon, P.C., and Tannenbaum, S.R. (2004). Reactive nitrogen species in the chemical biology of inflammation. Arch. Biochem. Biophys. *423*, 12–22.
5. Burney, S., Tamir, S., Gal, A., and Tannenbaum, S.R. (1997). A mechanistic analysis of nitric oxide-induced cellular toxicity. Nitric Oxide *1*, 130–144.
6. Marletta, M.A., and Spiering, M.M. (2003). Trace elements and nitric oxide function. J. Nutr. *133*, 1431S–1433S.
7. Ohshima, H., and Bartsch, H. (1994). Chronic infections and inflammatory processes as cancer risk factors: possible role of nitric oxide in carcinogenesis. Mutat. Res. *305*, 253–264.
8. Kuper, H., Adami, H.O., and Trichopoulos, D. (2000). Infections as a major preventable cause of human cancer. J. Intern. Med. *248*, 171–183.
9. Juedes, M.J., and Wogan, G.N. (1996). Peroxynitrite-induced mutation spectra of pSP189 following replication in bacteria and in human cells. Mutat. Res. *349*, 51–61.
10. Routledge, M.N. (2000). Mutations induced by reactive nitrogen oxide species in the *supF* forward mutation assay. Mutat. Res. *450*, 95–105.
11. Tamir, S., Burney, S., and Tannenbaum, S.R. (1996). DNA damage by nitric oxide. Chem. Res. Toxicol. *9*, 821–827.
12. West, S.C. (2003). Molecular views of recombination proteins and their control. Nat. Rev. Mol. Cell Biol. *4*, 435–445.
13. McGlynn, P., and Lloyd, R.G. (2002). Recombinational repair and restart of damaged replication forks. Nat. Rev. Mol. Cell Biol. *3*, 859–870.
14. Paques, F., and Haber, J.E. (1999). Multiple pathways of recombination induced by double-strand breaks in *Saccharomyces cerevisiae*. Microbiol. Mol. Biol. Rev. *63*, 349–404.
15. Morley, A.A., Grist, S.A., Turner, D.R., Kutlaca, A., and Bennett, G. (1990). Molecular nature of *in vivo* mutations in human cells at the autosomal *HLA-A* locus. Cancer Res. *50*, 4584–4587.
16. Shao, C., Deng, L., Henegariu, O., Liang, L., Raikwar, N., Sahota, A., Stambrook, P.J., and Tischfield, J.A. (1999). Mitotic recombination produces the majority of recessive fibroblast variants in heterozygous mice. Proc. Natl. Acad. Sci. USA *96*, 9230–9235.
17. Aubrecht, J., Rugo, R., and Schiestl, R.H. (1995). Carcinogens induce intrachromosomal recombination in human cells. Carcinogenesis *16*, 2841–2846.
18. Thompson, L.H., and Schild, D. (2002). Recombinational DNA repair and human disease. Mutat. Res. *509*, 49–78.
19. Bishop, A.J., and Schiestl, R.H. (2001). Homologous recombination as a mechanism of carcinogenesis. Biochim. Biophys. Acta *1471*, M109–M121.
20. Kang, M.H., Genser, D., and Elmadfa, I. (1997). Increased sister chromatid exchanges in peripheral lymphocytes of patients with Crohn's disease. Mutat. Res. *381*, 141–148.
21. Donovan, P.J., Smith, G.T., Lawlor, T.E., Cifone, M.A., Murli, H., and Keefer, L.K. (1997). Quantification of diazeniumdiolate mutagenicity in four different *in vitro* assays. Nitric Oxide *1*, 158–166.
22. Tanaka, R. (1997). Induction of a sister-chromatid exchange by nitrogen oxides and its prevention by SOD. J. Toxicol. Sci. *22*, 199–205.
23. Li, C.Q., Trudel, L.J., and Wogan, G.N. (2002). Nitric oxide-induced genotoxicity, mitochondrial damage, and apoptosis in human lymphoblastoid cells expressing wild-type and mutant p53. Proc. Natl. Acad. Sci. USA *99*, 10364–10369.
24. Dong, M., Wang, C., Deen, W.M., and Dedon, P.C. (2003). Absence of 2′-deoxyoxanosine and presence of abasic sites in DNA exposed to nitric oxide at controlled physiological concentrations. Chem. Res. Toxicol. *16*, 1044–1055.
25. Caulfield, J.L., Wishnok, J.S., and Tannenbaum, S.R. (1998). Nitric oxide-induced deamination of cytosine and guanine in deoxynucleosides and oligonucleotides. J. Biol. Chem. *273*, 12689–12695.
26. Nguyen, T., Brunson, D., Crespi, C.L., Penman, B.W., Wishnok, J.S., and Tannenbaum, S.R. (1992). DNA damage and mutation in human cells exposed to nitric oxide *in vitro*. Proc. Natl. Acad. Sci. USA *89*, 3030–3034.
27. Burney, S., Caulfield, J.L., Niles, J.C., Wishnok, J.S., and Tannenbaum, S.R. (1999). The chemistry of DNA damage from nitric oxide and peroxynitrite. Mutat. Res. *424*, 37–49.
28. deRojas-Walker, T., Tamir, S., Ji, H., Wishnok, J.S., and Tannenbaum, S.R. (1995). Nitric oxide induces oxidative damage in addition to deamination in macrophage DNA. Chem. Res. Toxicol. *8*, 473–477.
29. Kennedy, L.J., Moore, K., Jr., Caulfield, J.L., Tannenbaum, S.R., and Dedon, P.C. (1997). Quantitation of 8-oxoguanine and strand breaks produced by four oxidizing agents. Chem. Res. Toxicol. *10*, 386–392.
30. Yermilov, V., Rubio, J., and Ohshima, H. (1995). Formation of 8-nitroguanine in DNA treated with peroxynitrite *in vitro* and its rapid removal from DNA by depurination. FEBS Lett. *376*, 207–210.
31. Lee, J.C., Niles, J.S., Wishnok, J.S., and Tannenbaum, S.R. (2002). Peroxynitrite reacts with 8-nitropurines to yield 8-oxopurines. Chem. Res. Toxicol. *15*, 7–14.
32. Salgo, M.G., Stone, K., Squadrito, G.L., Battista, J.R., and Pryor, W.A. (1995). Peroxynitrite causes DNA nicks in plasmid pBR322. Biochem. Biophys. Res. Commun. *210*, 1025–1030.
33. Tretyakova, N.Y., Burney, S., Pamir, B., Wishnok, J.S., Dedon, P.C., Wogan, G.N., and Tannenbaum, S.R. (2000). Peroxynitrite-induced DNA damage in the *supF* gene: correlation with the mutational spectrum. Mutat. Res. *447*, 287–303.
34. Burney, S., Niles, J.C., Dedon, P.C., and Tannenbaum, S.R.

(1999). DNA damage in deoxynucleosides and oligonucleotides treated with peroxynitrite. Chem. Res. Toxicol. *12*, 513–520.
35. Tamir, S., deRojas-Walker, T., Wishnok, J.S., and Tannenbaum, S.R. (1996). DNA damage and genotoxicity by nitric oxide. Methods Enzymol. *269*, 230–243.
36. David, S.S., and Williams, S.D. (1998). Chemistry of glycosylases and endonucleases involved in base-excision repair. Chem. Rev. *98*, 1221–1262.
37. Chaudhry, M.A., and Weinfeld, M. (1995). The action of *Escherichia coli* endonuclease III on multiply damaged sites in DNA. J. Mol. Biol. *249*, 914–922.
38. Harrison, L., Hatahet, Z., Purmal, A.A., and Wallace, S.S. (1998). Multiply damaged sites in DNA: interactions with *Escherichia coli* endonucleases III and VIII. Nucleic Acids Res. *26*, 932–941.
39. Coquerelle, T., Dosch, J., and Kaina, B. (1995). Overexpression of N-methylpurine-DNA glycosylase in Chinese hamster ovary cells renders them more sensitive to the production of chromosomal aberrations by methylating agents—a case of imbalanced DNA repair. Mutat. Res. *336*, 9–17.
40. Sobol, R.W., Kartalou, M., Almeida, K.H., Joyce, D.F., Engelward, B.P., Horton, J.K., Prasad, R., Samson, L.D., and Wilson, S.H. (2003). Base excision repair intermediates induce p53-independent cytotoxic and genotoxic responses. J. Biol. Chem. *278*, 39951–39959.
41. Spek, E.J., Vuong, L.N., Matsuguchi, T., Marinus, M.G., and Engelward, B.P. (2002). Nitric oxide-induced homologous recombination in *Escherichia coli* is promoted by DNA glycosylases. J. Bacteriol. *184*, 3501–3507.
42. Yang, N., Galick, H., and Wallace, S.S. (2004). Attempted base excision repair of ionizing radiation damage in human lymphoblastoid cells produces lethal and mutagenic double strand breaks. DNA Repair (Amst.) *3*, 1323–1334.
43. Wang, C., and Deen, W.M. (2003). Nitric oxide delivery system for cell culture studies. Ann. Biomed. Eng. *31*, 65–79.
44. Jonnalagadda, V., Matsuguchi, T., and Engleward, B.P. (2005). Interstrand corsslink-induced homologous recombination carries increased risk of deletions and insertions. DNA Repair, in press.
45. Hendricks, C.A., Almeida, K.H., Stitt, M.S., Jonnalagadda, V.S., Rugo, R.E., Kerrison, G.F., and Engelward, B.P. (2003). Spontaneous mitotic homologous recombination at an enhanced yellow fluorescent protein (EYFP) cDNA direct repeat in transgenic mice. Proc. Natl. Acad. Sci. USA *100*, 6325–6330.
46. Bill, C.A., and Nickoloff, J.A. (2001). Spontaneous and ultraviolet light-induced direct repeat recombination in mammalian cells frequently results in repeat deletion. Mutat. Res. *487*, 41–50.
47. Sonoda, E., Sasaki, M.S., Morrison, C., Yamaguchi-Iwai, Y., Takata, M., and Takeda, S. (1999). Sister chromatid exchanges are mediated by homologous recombination in vertebrate cells. Mol. Cell. Biol. *19*, 5166–5169.
48. Mudgett, J.S., and Taylor, W.D. (1990). Recombination between irradiated shuttle vector DNA and chromosomal DNA in African green monkey kidney cells. Mol. Cell. Biol. *10*, 37–46.
49. Slebos, R.J., and Taylor, J.A. (2001). A novel host cell reactivation assay to assess homologous recombination capacity in human cancer cell lines. Biochem. Biophys. Res. Commun. *281*, 212–219.
50. Tretyakova, N.Y., Wishnok, J.S., and Tannenbaum, S.R. (2000). Peroxynitrite-induced secondary oxidative lesions at guanine nucleobases: chemical stability and recognition by the Fpg DNA repair enzyme. Chem. Res. Toxicol. *13*, 658–664.
51. Taghian, D.G., and Nickoloff, J.A. (1997). Chromosomal double-strand breaks induce gene conversion at high frequency in mammalian cells. Mol. Cell. Biol. *17*, 6386–6393.
52. Sargent, R.G., Brenneman, M.A., and Wilson, J.H. (1997). Repair of site-specific double-strand breaks in a mammalian chromosome by homologous and illegitimate recombination. Mol. Cell. Biol. *17*, 267–277.
53. Lechardeur, D., Sohn, K.J., Haardt, M., Joshi, P.B., Monck, M., Graham, R.W., Beatty, B., Squire, J., O'Brodovich, H., and Lukacs, G.L. (1999). Metabolic instability of plasmid DNA in the cytosol: a potential barrier to gene transfer. Gene Ther. *6*, 482–497.
54. Tanswell, A.K., Staub, O., Iles, R., Belcastro, R., Cabacungan, J., Sedlackova, L., Steer, B., Wen, Y., Hu, J., and O'Brodovich, H. (1998). Liposome-mediated transfection of fetal lung epithelial cells: DNA degradation and enhanced superoxide toxicity. Am. J. Physiol. *275*, L452–L460.
55. Parsons, J.L., and Elder, R.H. (2003). DNA N-glycosylase deficient mice: a tale of redundancy. Mutat. Res. *531*, 165–175.
56. Bishop, A.J., and Schiestl, R.H. (2003). Role of homologous recombination in carcinogenesis. Exp. Mol. Pathol. *74*, 94–105.
57. Stuehr, D.J., and Marletta, M.A. (1987). Synthesis of nitrite and nitrate in murine macrophage cell lines. Cancer Res. *47*, 5590–5594.
58. Lewis, R.S., Tamir, S., Tannenbaum, S.R., and Deen, W.M. (1995). Kinetic analysis of the fate of nitric oxide synthesized by macrophages *in vitro*. J. Biol. Chem. *270*, 29350–29355.
59. Lymar, S.V., Jiang, Q., and Hurst, J.K. (1996). Mechanism of carbon dioxide-catalyzed oxidation of tyrosine by peroxynitrite. Biochemistry *35*, 7855–7861.
60. Doulias, P.T., Barbouti, A., Galaris, D., and Ischiropoulos, H. (2001). SIN-1-induced DNA damage in isolated human peripheral blood lymphocytes as assessed by single cell gel electrophoresis (comet assay). Free Radic. Biol. Med. *30*, 679–685.
61. Li, C.Q., Trudel, L.J., and Wogan, G.N. (2002). Genotoxicity, mitochondrial damage, and apoptosis in human lymphoblastoid cells exposed to peroxynitrite generated from SIN-1. Chem. Res. Toxicol. *15*, 527–535.
62. Smith, S.A., and Engelward, B.P. (2000). *In vivo* repair of methylation damage in Aag 3-methyladenine DNA glycosylase null mouse cells. Nucleic Acids Res. *28*, 3294–3300.
63. Wuenschell, G.E., O'Connor, T.R., and Termini, J. (2003). Stability, miscoding potential, and repair of 2′-deoxyxanthosine in DNA: implications for nitric oxide-induced mutagenesis. Biochemistry *42*, 3608–3616.
64. Wilson, D.M., 3rd, Sofinowski, T.M., and McNeill, D.R. (2003). Repair mechanisms for oxidative DNA damage. Front. Biosci. *8*, 963–981.
65. Fromme, J.C., Banerjee, A., and Verdine, G.L. (2004). DNA glycosylase recognition and catalysis. Curr. Opin. Struct. Biol. *14*, 43–49.
66. Wilson, D.M., III, Engelward, B.P., and Samson, L. (1998). Prokaryotic Base Excision Repair. In DNA Damage and Repair: Biochemistry, Genetics, and Cell Biology, Volume I,, J.A. Nickoloff and M.F. Hoekstra, eds. (Totowa, NJ: Humana Press Inc.), pp. 29–64.
67. Winn, L.M., Kim, P.M., and Nickoloff, J.A. (2003). Oxidative stress-induced homologous recombination as a novel mechanism for phenytoin-initiated toxicity. J. Pharmacol. Exp. Ther. *2*, 523–527.
68. Sandberg, A.A. (1982). Sister Chromatid Exchange (New York: Alan R. Liss, Inc.).
69. Okabe, M., Ikawa, M., Kominami, K., Nakanishi, T., and Nishimune, Y. (1997). 'Green mice' as a source of ubiquitous green cells. FEBS Lett. *407*, 313–319.
70. Pryor, W.A., Cueto, R., Jin, X., Koppenol, W.H., Ngu-Schwemlein, M., Squadrito, G.L., Uppu, P.L., and Uppu, R.M. (1995). A practical method for preparing peroxynitrite solutions of low ionic strength and free of hydrogen peroxide. Free Radic. Biol. Med. *18*, 75–83.
71. Lindahl, T., and Andersson, A. (1972). Rate of chain breakage at apurinic sites in double-stranded deoxyribonucleic acid. Biochemistry *11*, 3618–3623.
72. Kim, M.Y., Dong, M., Dedon, P.C., and Wogan, G.N. (2005). Effects of peroxynitrite dose and dose-rate on DNA damage and mutation in the supF shuttle vector. Chem. Res. Toxicol. *18*, 76–86.